Journal of Electronic Materials (2024) 53:5103–5117
https://doi.org/10.1007/s11664-024-11168-9

28TH INTERNATIONAL CONFERENCE ON NUCLEAR TRACKS AND RADIATION MEASUREMENTS

PANI/CD/SnO_2 Ternary Nanocomposite for Efficient Room-Temperature Ammonia Detection

Jiya[1] · Shiv Dutta Lawaniya[1] · Gaurav Pandey[1] · Nishel Saini[1] · Kamlendra Awasthi[1]

Received: 12 February 2024 / Accepted: 6 May 2024 / Published online: 25 May 2024

Abstract

We report a unique combination of three components in the form of a ternary nanocomposite, PANI/CD/SnO_2, for ammonia gas sensing at room temperature. This nanocomposite was synthesized via in situ chemical oxidative polymerization of aniline, in which other components were incorporated to form binary PANI/CD and ternary PANI/CD/SnO_2 nanocomposites. The fabrication process initially involved optimization of the PANI/CD nanocomposite and then incorporation of an optimized amount of SnO_2 to finally produce the ternary PANI/CD/SnO_2 nanocomposite. The ternary composite demonstrated better sensing properties than those of both PANI/CD (1:0.5) and pristine PANI in terms of sensitivity, selectivity, and response time over a concentration range of 5–100 ppm NH_3. The response of the PANI/CD/SnO_2 nanocomposite was 21.6% towards 100 ppm NH_3, which was higher than that of pure PANI and the PANI/CD nanocomposite. The ternary composite exhibited higher selectivity for ammonia over other gases as compared to PANI and the PANI/CD (1:0.5) nanocomposite. The PANI/CD/SnO_2 composite also achieved a shorter response time (94 s) than pure PANI (162 s) and the PANI/CD (144 s) composite, and it demonstrated a nearly linear variation in response with the analyte concentration. High repeatability and long-term stability further enhanced the possibility of real-world application of the proposed ternary nanocomposite for practical room-temperature ammonia sensing.

Keywords Polyaniline (PANI) · carbon dots (CD) · tin oxide (SnO_2) · ammonia gas sensing · ternary composite

Introduction

Population growth and urbanization are directly related to the depletion of natural resources and relative imbalance in environmental parameters, with detrimental effects. For instance, the overuse of conventional energy sources, excessive use of nitrogen-containing fertilizer in agricultural fields, and effluent release in various industries (during production of fertilizers, plastics, textiles, rubber, cement, and as bleaching agents)[1,2] lead to air, water, and soil pollution. All these activities increase the concentration of ammonia in the immediate surroundings as well as in the atmosphere, exceeding the critical concentration. As a consequence, adverse effects are experienced by both flora and fauna, particularly humans who are exposed to high concentrations of the gas in those industries, or in highly populated or industrial areas or while working in agricultural lands.[3] Exposure to ammonia gas in concentrations exceeding the critical limit results in harm to the respiratory system and acute pulmonary congestion, in addition to damage to eyes, skin, neural system, and digestive system.[4–6] Therefore, gas sensing is an important technology that needs to advance with the advancement of other technologies and urbanization.[7,8]

With the increased need for ammonia gas sensing, research on the development of gas sensors has accelerated. Initially, semiconductor metal oxides and their composites (e.g. ZnO, SnO_2, TiO_2, WO_3, Fe_2O_3, Co_3O_4) were primarily used for gas sensing material synthesis.[9] With time, conducting polymers (e.g. polyaniline [PANI], polypyrrole [PPy], polythiophene [PTH], poly(3,4-ethylenedioxythiophene) [PEDOT], polyphenylene vinylene [PPV], polystyrene) and carbon-based materials (e.g. graphene, carbon nanotubes, reduced graphene oxide) have gained attention in the

✉ Kamlendra Awasthi
kawasthi.phy@mnit.ac.in

[1] Department of Physics, Malaviya National Institute of Technology Jaipur, Jaipur, Rajasthan 302017, India

field of gas sensing.[3,4,10,11] Conducting polymers in nanostructure form have been extensively used for gas sensing because of their electrical and optical properties (comparable to metal and inorganic semiconductors) along with very good mechanical properties, high surface-to-volume ratio, and light weight. They also demonstrate ease of functionalization[12] and hybrid/composite formation with other material, less power consumption, low cost, ability to change conductivity, surface modification, good redox properties, and unique electrical transduction mechanism, which aid in good sensing performance at room temperature.[3,13,14] PANI is an important conducting polymer that is utilized extensively as a sensing material. This is because of its advantages over other conducting polymers such as good electrical properties, high reliability, better electrical conductivity, ease of synthesis, high flexibility, high sensitivity, and low production cost. Environmental stability, large surface area, and pH sensitivity of PANI are beneficial for fabrication of sensors.[15,16]

Conducting polymers when used in pristine form also suffer some limitations such as instability towards moisture and high temperature, reduced performance with long exposure time to air, and less stability and selectivity. To enhance performance, metal oxides and/or carbon-based materials are incorporated into conducting polymers to form nanocomposites. These nanocomposites function efficiently at room temperature, offering improved flexibility and enhancing sensitivity, selectivity, stability, and speed.[17,18] Hence, conducting polymers of different morphology and binary or ternary nanocomposites of conducting polymers are currently being explored for the development of gas sensors and for all the applications of gas sensing.

Carbon-based nanomaterials are also important in sensing, owing to their properties including high surface-to-volume ratio, good electrical properties, environmentally friendly nature, flexibility, high carrier density and mobility (in graphene), and high mechanical strength and flexibility (in carbon nanotubes [CNT)]).[19–21] Various carbon-based materials have been used to functionalize conducting polymers. For instance, Lawaniya et al. reported a binary composite PPy-CNT for room-temperature sensing of ammonia gas. They synthesized different PPy-CNT nanocomposite samples via in situ and ex situ methods by varying the amount of CNTs. The in situ-synthesized samples responded better than ex situ-synthesized samples and pure PPy. The sensor demonstrated high selectivity towards NH_3 as compared to H_2, CO_2, and C_2H_5OH.[4] Another room-temperature ammonia gas sensor was reported by Hong et al. based on PANI/hollow C# In_2O_3 nanofibre (NF) composite. The nanocomposite of PANI/hollow C# In_2O_3 NF achieved a better response than PANI and PANI/hollow In_2O_3 NF (1.6 times higher) and was highly selective for ammonia.[22] These examples highlight the potential for incorporating carbon materials into a conducting polymer matrix to enhance the sensing performance of the synthesized nanocomposite relative to its components in pure form.[23]

Carbon-based materials of one and two dimensions, i.e. CNT (1D),[24,25] rGO (2D),[26,27] and graphene (2D),[28,29] have been studied as possible sensing materials for many gases including ammonia gas. Carbon dots, an important 0D carbon-based material, are gaining attention today for use as sensing material. The enhanced sensing properties of quantum dots of any material, in general, include tunability of the band gap (i.e. electrical properties) via size control, low power consumption, and high adsorption of molecules due to a high surface-to-volume ratio. Due to their small size (smaller than the Debye length), the entire quantum dot forms the depletion layer, and hence the resistive response is higher.[30–34] There have been recent reports of carbon dot-based nanocomposites for gas sensing purpose. For instance, Hakimi et al. reported a graphene quantum dot (GQD)-based sensor synthesized using N-doped GQDs/PANI (50 wt.%) for sensing ammonia at room temperature,[32] and the nanocomposite yielded a much higher response than pure PANI. The increase in response is attributed to an increase in porosity in the nanocomposite upon incorporation of GQDs into the polyaniline matrix. It has been reported that there are a higher number of surface active sites on graphene in order to accommodate PANI molecules.[29] A S,N:GQDs/PANI hybrid gas sensor was reported by Gavgani et al. for ammonia gas sensing. The hybrid sensor demonstrated a significantly better response than pure PANI. This indicates the benefit of the nanocomposite of S,N-co-doped GQDs with PANI, in terms of the synergistic interaction of individual PANI (via redox reaction) and S,N:GQDs (via *p*-type behaviour). Also, the increase in resistance of the S,N:GQDs/PANI hybrid when exposed to NH_3 gas is attributed to an additional factor which is the swelling process due to diffusion of NH_3 molecules.[33] For practical purposes, we require a material with a high response as well as a shorter response and recovery time and enhanced stability against high temperature and moisture conditions. Both of the abovementioned sensing materials exhibit long response time and a significantly lower response relative to the gas concentration exposed. Hence, in order to resolve the issues with the current sensing materials and further improve the sensing parameters, research is increasingly focusing on ternary composites composed of the most effective materials currently used for sensing applications. Among the most investigated are different types of metal oxides such as ZnO, SnO_2, TiO_2, WO_3, Fe_2O_3, and Co_3O_4, which are used for gas sensing applications due to their easy production, low cost, fast response, good sensitivity, and compact size. Ternary nanocomposites have emerged as improved sensing materials for better sensitivity and higher selectivity and stability, with faster response and recovery. Therefore, an analysis of the advantages and

disadvantages in each type of sensing material, metal oxides, carbon-based materials, and conducting polymers, has provided the motivation to create ternary nanocomposites. These combinations are designed such that the advantages of one material compensates for the limitations of another. For example, the poor responsiveness of metal oxides at high temperature is overcome by the room-temperature sensing ability of a conducting polymer,[22,35] whereas the high stability of carbon nanomaterials[10,24,36] counters the poor stability of conducting polymers and metal oxides, ultimately leading to overall high stability of a ternary nanocomposite from these materials. Also, metal oxides can aid in reducing the response time and increase the response, which is higher in the case of conducting polymers.[10,35,37] One such composite was reported by Hong et al., who prepared a PANI/N-GQD/hollow In_2O_3 nanofibre ternary composite which yielded a response of 15.1 (R_g/R_a) towards 1 ppm NH_3, which was 4.4 times and 1.4 times higher than the response of pure PANI and PANI/hollow In_2O_3 nanofibre. Their sensor was found to be selective towards ammonia against methanol, ethanol, acetone, and hexane. Heterojunction formation between *p*-type PANI and *n*-type N-GQD-coated hollow In_2O_3 nanofibres was thought to be the reason for the improvement, thereby providing a synergistic effect of all three components.[38]

Among the different metal oxides, tin oxide (SnO_2) has been a great option as sensing material,[39–41] as its morphology can be tuned by synthesis, for example, to form hollow spheres, nanospheres, nanowires, or nanotubes. However, a major problem with SnO_2 is a deterioration in response over the long term due to poor stability. Also, selectivity is an issue with SnO_2. It is operational at very high temperatures, posing a problem for fabrication of sensor devices, and hence increasing the cost. A PPy/SnO_2/graphene nanoribbon (GNR) nanocomposite as reported by Hsieh et al. is an example of improved sensor fabrication where ternary nanocomposites are used. The nanocomposite (with 3 wt.% of SnO_2) exhibited a high response even towards low concentrations of NH_3. It was found to be selective for ammonia against methanol, ethanol, and acetone. The combination of *n*-type SnO_2 nanoparticles with PPy-coated GNR is responsible for the synergistic effect, and thus the sensitivity is enhanced by p–n heterojunction formation. Also, the SnO_2 and GNR surfaces have oxygen-containing defects on which covalent bonds can be formed. The high surface area of SnO_2 and GNR further increases the adsorption sites for ammonia. A high response time was observed.[39]

This paper explores the incorporation of different amounts of carbon dots (CDs) (aniline-to-CD ratios of 1:1, 1:0.5, and 1:2) into a PANI conducting polymer matrix via in situ polymerization, which forms a PANI/CD nanocomposite. The nanocomposite sample was optimized for the amount of CDs by investigating its sensing response towards ammonia gas at room temperature, which revealed that the optimized sample was the 1:0.5 PANI/CD nanocomposite. In order to further enhance the sensing parameters, synthesis of ternary nanocomposites was carried out by incorporating 20 wt.% SnO_2 nanorods along with CDs (in an optimized ratio of 1:0.5) during in situ polymerization of aniline to form a PANI/CD/SnO_2 nanocomposite. Gas sensing measurements of the composite towards NH_3 gas at room temperature exhibited higher response and selectivity and lower response time than that of the pristine PANI and binary composites. Also, the sensor was experimentally observed to exhibit high repeatability and long-term stability. Characterization techniques including scanning electron microscopy (SEM), Fourier transform infrared (FTIR) spectroscopy, x-ray diffraction, and Raman spectroscopy were exploited to ensure the successful incorporation and the interaction of CDs and SnO_2 nanorods with polyaniline nanofibres. All results demonstrated high interaction in both binary and ternary nanocomposites. To the best of our knowledge, this is the first study to report a ternary nanocomposite of PANI/CD/SnO_2 combining all three components used for ammonia gas sensing. Hence, this new sensing material can serve as a practical ammonia gas sensor with good sensing parameters.

Experimental Section

Materials

Citric acid ($C_6H_8O_7.H_20$, 99.5 + %, Alfa Aesar), urea crystal (NH_2CONH_2, 99%, CDH), formamide (CH_3NO, 98.5%, CDH), hydrochloric acid (HCl, 37%, Merck), aniline ($C_6H_5NH_2$, Merck), ammonium persulphate (APS) ($(NH_4)2S_2O_8$, 98%, Loba Chemie Pvt. Ltd.), tin(IV) chloride pentahydrate ($SnCl_4.5H_2O$, 98%, HiMedia Laboratories Pvt. Ltd.), and sodium hydroxide pellets (NaOH, 97%, Thermo Fisher Scientific India Pvt. Ltd.) were used for synthesis in this paper. The chemicals used were of analytical grade and used as received with no further purification. An ammonia gas cylinder of 1000 ppm volume was purchased from Ankur Gases, India.

Synthesis Methods

Synthesis of Carbon Dots (CDs)

Carbon dots were synthesized using a solvothermal method as reported by Holá et al.[42] First, 4 g citric acid and 4 g urea were dissolved in 60 mL formamide and mildly ultrasonicated for uniform dissolution of salts in the solvent. The prepared solution was transferred to an 80 mL Teflon cup of a hydrothermal vessel, which was placed in a preheated oven at 180°C for 12 h to induce the solvothermal reaction for the

synthesis of the nanomaterial. The resulting dark red mixture indicated the successful formation of carbon quantum dots.

Synthesis of Polyaniline (PANI)

Polyaniline nanofibres were synthesized using chemical oxidative polymerization of aniline as reported by Kaur et al.[37] The process, as described in Fig. 1, was carried out as follows. First, 10 mL of 1 M HCl solution was prepared in each of two 15 mL glass vials, after which 0.3 mL aniline was added to one of the vials and 0.18 g APS to the other. The contents of both vials were then rapidly combined in a 30 mL glass vial and shaken vigorously for 30 s, and the mixture was left for 2 h for static polymerization to occur. Following the reaction, the product was washed with 200 mL of 0.1 M HCl, followed by deionized (DI) water and acetone alternately until a pH of 7 was obtained. Finally, the product was dried at 60°C, and pristine PANI was obtained in powder form.

Synthesis of Tin Oxide (SnO_2)

Synthesis of the SnO_2 nanorods was performed utilizing a hydrothermal method as reported by Pandey et al.[43] First, 1.33 g $SnCl_4.5H_2O$ (stannic chloride pentahydrate) was dissolved in 25 mL of 1.26 M NaOH solution by stirring for 10 min. Next, 25 mL of absolute ethanol was added to the solution, followed by further stirring until a white transparent suspension was obtained. The solution was then transferred to an 80 mL stainless steel autoclave and placed in an oven at 200°C for 24 h to induce the solvothermal reaction at high temperature and high pressure. After the reaction was completed, the solution was allowed to cool to room temperature. The reaction solution was then washed with DI water and ethanol alternately to remove any impurities, and finally dried at 60°C for 24 h.

Synthesis of PANI/CD and PANI/CD/SnO_2 Composites

In situ synthesis was employed for fabrication of the PANI/CD nanocomposite by incorporating the CD solution during the chemical oxidative polymerization of aniline. This process, as shown in Fig. 1, is explained as follows. Initially, 10 mL of 1 M HCl solution is prepared in each of two 15 mL glass vials. To one vial, 0.3 mL aniline is added, while 0.18 g APS is added to the other. The synthesized CDs are added into the vial with aniline, in three different ratios of aniline:CD, namely 1:1, 1:0.5, and 1:2. The mixture is ultrasonicated for 20 min. The contents of both vials are then rapidly combined in a 30 mL glass vial and shaken vigorously for 30 s. The mixture is then left for 2 h for static polymerization to occur. Following the reaction, the product is washed with 200 mL of 0.1 M HCl, followed by DI water and acetone alternately until a pH of 7 is obtained. Finally, the product is dried at 60°C, and the nanocomposite is obtained in powder form. For synthesis of PANI/CD/SnO_2, a similar method was executed but 20 wt.% of SnO_2, as optimized in the lab, was added to the vial of aniline with 0.15 mL of CDs. The optimized ratio in the present paper is 1:0.5 aniline:CD. Other steps are the same as mentioned in the above method.

Characterization

Scanning electron microscopy (SEM) (Nova NanoSEM 450, FEI) was employed for analysis of the surface of the synthesized ternary composite. To understand the crystallographic structure of the PANI/CD/SnO_2 nanocomposite, x-ray diffraction (XRD) was performed (Panalytical X'Pert Pro diffractometer) using CuK_α radiation. Fourier transform infrared spectroscopy (FTIR, PerkinElmer)) was used to study the different chemical bonds present inside the synthesized samples. Raman spectroscopy of all samples including the ternary nanocomposite was performed on a Renishaw spectrometer. To analyse the absorbance of the synthesized samples, UV–Vis

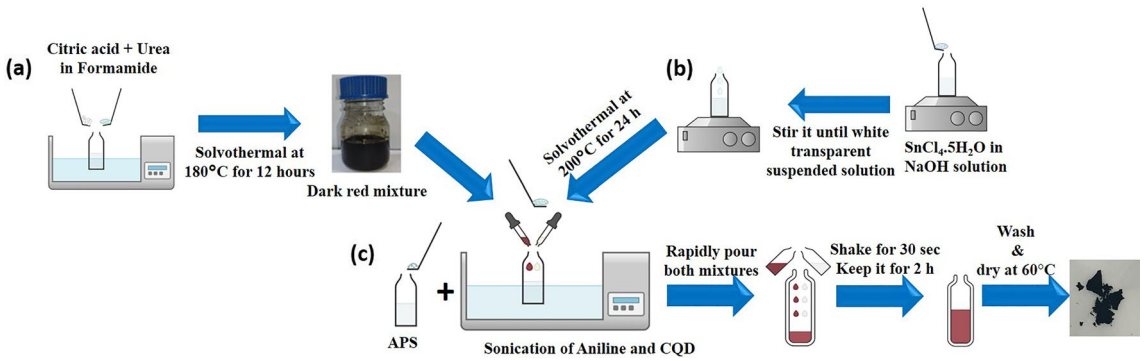

Fig. 1 Schematic of synthesis procedure for (a) CDs, (b) SnO_2 nanorods, and (c) PANI/CD/SnO_2 nanocomposite.

spectroscopy was performed using a UV–Vis spectrometer (Agilent Technologies)

Gas Sensor Fabrication and Measurements

For the gas sensing measurements, interdigitated electrodes (IDEs) of aluminium deposited over a SiO_2 substrate were employed. The synthesized samples were first ground using a mortar and pestle, and then using only a few drops of alpha-terpinol, a thick slurry was made from the ground powder. The IDEs were then coated and used for gas sensing measurements after drying at room temperature. All the sensing measurements were performed at room temperature using a two-probe measurement technique. The experimental setup basically comprised a closed chamber of fixed volume, consisting of a sample stage with a controlled heating system, connected to a vacuum pump to first remove all the undesired gases and for recovery of the sample by pumping out the specific gas and letting in air. The flow of gas of a particular concentration was controlled through a syringe system. The experiment was carried out using a LabView programme specifically designed for high-resistance gas sensing measurements, which measures the change in the resistance of the sensing material/sample when exposed to a specific gas and then recovery during air flow after expulsion of the gas. Finally, the sensing response of the material for that particular gas is calculated using the formula

$$R(\%) = \frac{R_g - R_a}{R_a} \times 100 \quad (1)$$

Results and Discussion

Material Characterization Analysis

In situ synthesis was purposefully employed to ensure the proper incorporation and interaction of all the individual components for effective synergistic effects of the ternary nanocomposite to accomplish better sensing. Various characterization techniques were used to confirm the successful synthesis of the ternary nanocomposite.

Scanning electron microscopy (SEM) is an important characterization technique that makes it possible to visualize the surface morphology of the synthesized composite as well its components. SEM of the ternary PANI/CD/SnO_2 nanocomposite, as shown in Fig. 2, clearly indicates uniform distribution of SnO_2 nanorods on and around chains of polyaniline. As CDs are very small in size, they are not visible, and may also be expected to be present deep inside hollow spaces in the numerous PANI and SnO_2 nanorods (assembled in the form of nanoflowers). PANI nanofibres formed around small carbon dots or entangled around carbon dots are further seen to form chain-like structures on and around SnO_2 nanorods, which ensures a high number of inter-junctions and cross-connections between the PANI nanofibres containing CDs and SnO_2 nanorods. By analysis of Fig. 2, it can be inferred that SnO_2 nanorods arranged in the form of nanoflowers contribute to an increase in the net surface area relative to PANI/CD and PANI nanofibres, as we incorporated SnO_2 nanorods and CDs at the time of polymerization of aniline to form polyaniline (PANI). Hence, SnO_2 nanorods and CD must act as seeds for polymerization, resulting in the formation of nanofibres on and around SnO_2 nanoflowers, thereby increasing the spacing between nanofibres and hence enhancing the porosity relative to the porosity when only aniline was polymerized or when only CDs were incorporated during polymerization. The small size

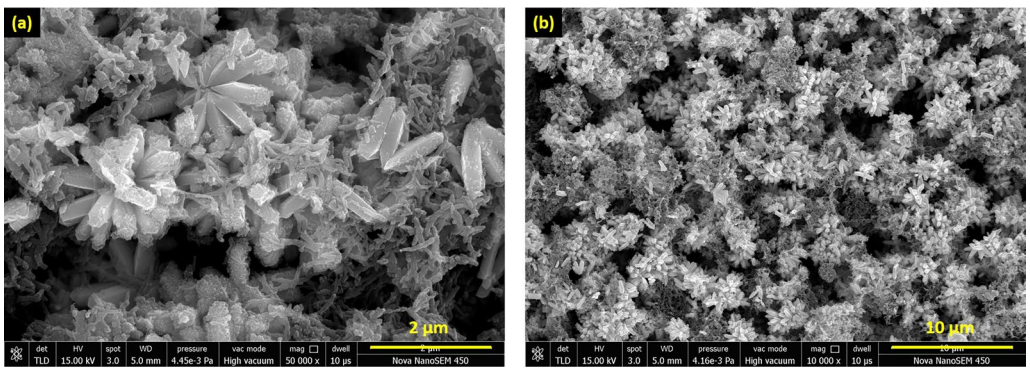

Fig. 2 (a) High- and (b) low-magnification SEM image of the ternary PANI/CD/SnO_2 nanocomposite.

of CDs alone would not significantly increase the spacing between nanofibres, leading to less porosity than in ternary nanocomposites in which SnO_2 nanoflowers (of considerably larger size) were incorporated along with CDs. This can also be directly related to the increase in surface area after incorporation of SnO_2 nanoflowers relative to the surface area before adding them. This is due to the incorporation of an additional component, i.e. SnO_2 nanorods, which are arranged in the form of nanoflowers, resulting in a morphology with a high surface area. Also, the increase in spacing between nanofibres leads to an increase in surface area in ternary nanocomposites as compared to pure PANI and the PANI/CD nanocomposite.

Energy-dispersive x-ray spectroscopy (EDX) spectroscopy is another characterization technique that is generally used to examine the elemental composition of a compound or material, and also indicates the relative amount of each element. The EDX spectrum of the ternary PANI/CD/SnO_2 nanocomposite clearly indicates the presence of Sn, C, O, N, and Cl atoms, as expected due to the presence of tin oxide nanorods, carbon dots (synthesized using citric acid and urea), and polyaniline (synthesized using HCl acid) (see supplementary Fig. S1).

Information about the crystal structure of a material/sample is obtained using x-ray diffraction, which gives information about the planes present and hence the lattice of the sample. The XRD spectra for the ternary PANI/CD/SnO_2 nanocomposite are shown in Fig. 3a. We can observe some very high-intensity peaks at 26.95° (110), 34.25° (101), 38.21° (200), 39.36° (111), 52.03° (211), 54.98° (220), 58.29° (002), 62° (310), 65.07° (112), 66.23° (301), 71.72° (202), and 78.89° (321) which are characteristic of SnO_2 but are slightly displaced from their reported positions as given in JCPDS card number 00-003-0439. The reported peak positions are plotted in the lower plot in Fig. 3a along with the altered peak positions in the upper graph, which also indicates a new broad peak at 20.54°. The slight displacement in peak positions can be attributed to the interaction between SnO_2 nanorods, PANI nanofibres, and carbon dots, which may cause some disturbance to the structure of SnO_2 nanorods as compared to pure SnO_2. These peaks correspond to their respective planes[43] as marked in the figure.

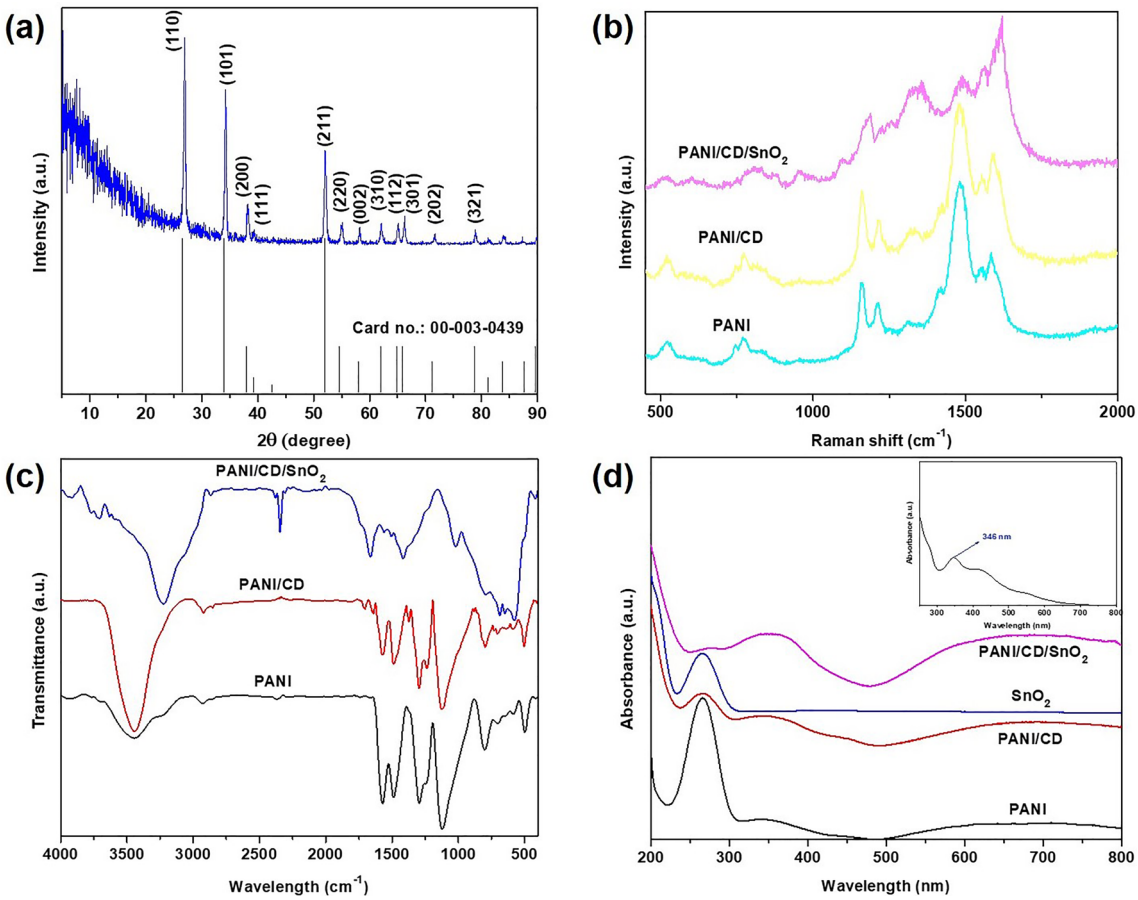

Fig. 3 (a) XRD pattern of PANI/CD/SnO_2 nanocomposite. (b) Raman spectra, (c) FTIR spectra, and (d) UV–Vis spectra of pure PANI, PANI/CD (1:0.5), and the PANI/CD/SnO_2 nanocomposite.

One can observe a broad peak at 20.54° confirming the amorphous nature of the PANI nanofibres.[42,44] Carbon dots exhibit poor crystallinity as reported in JCPDS card number 26-1076, contributing to the broad peak at 20.54°.[45] Hence, XRD spectra confirm the successful synthesis of an effectively interacting ternary PANI/CD/SnO_2 nanocomposite.

In order to analyse the vibration mode of the molecules present in the composite through the identification of the molecular fingerprint and hence of the nanocomposites and their interactions, Raman spectroscopy was performed for the three samples—pure PANI, PANI/CD (1:0.5), and PANI/CD/SnO_2. The Raman spectra for these samples are shown in Fig. 3b. The spectra of PANI possess all the prominent peaks characteristics of PANI, as reported in the literature. Less intense peaks are observed at 521.5 cm^{-1}, corresponding to in-plane deformation of amine, and at 745.69 cm^{-1} and 770.8 cm^{-1}, corresponding to deformation of the imine and quinoid groups.[46] Peaks at 1160 cm^{-1} and 1213.05 cm^{-1} indicate in-plane bending vibrations of the C–H bond of quinone rings[46,47] and stretching deformation of the C–N bond in the amine group of PANI.[46,47] The most intense peaks are present at 1481.7 cm^{-1}, representing stretching vibrations of the C=N bond in imine,[47] along with three smaller peaks at 1419.9 cm^{-1}, 1550.74 cm^{-1}, and 1585.4 cm^{-1}, corresponding to stretching of the C=N bond, bending of the N–H bond, and stretching of the C=C bond (in the quinoid group), respectively.[46] A peak of much lower intensity at 1309.82 cm^{-1} represents stretching of the C–N^+ bond (shifted slightly from normal positional range).[48] Upon comparing the spectra for the pure PANI and PANI/CD nanocomposite, one can clearly observe that all the peaks present in PANI are at nearly the same positions, and only two peaks have changed in intensity and slightly in position due to the presence of CDs. The synthesized carbon dots show two peaks at 1340 cm^{-1} and 1590 cm^{-1},[42] due to which the 1309 cm^{-1} and 1585.4 cm^{-1} peaks of pure PANI seen earlier have shifted to 1333.28 cm^{-1} and 1591.7 cm^{-1}, respectively, with increased intensity. This confirms the incorporation of CDs into PANI. The successful formation of SnO_2 can be confirmed via the presence of new peaks along with changes in intensity and positions of the peaks corresponding to PANI and CDs. This indicates the desired interaction between the three components of the PANI/CD/SnO_2 nanocomposite. As the morphology of the composite is such that PANI nanofibres (around CDs) are present on and around SnO_2 nanorods, the interaction of this composite with radiation cannot be considered to be with each component individually, but with the integration of all three components interacting with each other, as a result of which we obtain a different pattern in the spectra of the ternary composite.

FTIR spectroscopy was performed for all three synthesized samples to examine the bonds present in the molecules or compound and their respective vibrations. FTIR spectroscopic measurements for PANI, PANI/CD (1:0.5), and PANI/CD/SnO_2 are presented in Fig. 3c. The spectra for pure PANI display all the prominent peaks similar to those reported in previous papers. These are 3439 cm^{-1}, 2926 cm^{-1}, 1568 cm^{-1}, 1487 cm^{-1}, 1294 cm^{-1}, 1120 cm^{-1}, 802 cm^{-1}, and 499 cm^{-1}, which correspond to different respective bonds present in PANI. The peak at 3439 cm^{-1} represents N–H bond vibrations,[49] and the peak at 2926 cm^{-1} corresponds to asymmetric C–H stretching vibrations.[50] The peaks at 1568 and 1487 cm^{-1} are related to stretching vibrations of quinonoid and benzenoid rings, respectively.[50] The peak at 1294 cm^{-1} is attributed to stretching vibrations of the C–N bond,[49] while those at 1120 and 802 cm^{-1} represent C–N stretching vibrations for benzenoid rings and C–H bonds executing plane bending vibrations, respectively.[50] The FTIR spectra of PANI/CD (1:0.5) show all the peaks that were present in pure PANI but with some peaks slightly shifted. An additional peak at 1707 cm^{-1} is obtained in PANI/CD (1:0.5) as compared to pure PANI, which can be attributed to a peak in the synthesized CDs at 1710 cm^{-1}, representing the C=O bond, as reported in the paper from which the synthesis method was taken.[42] Also, the paper reports a peak at 1600 cm^{-1} for the C=C bond, which is noted to be shifted in the spectra of PANI/CD to 1641 cm^{-1}.[42] The shift in peaks as well as the new peaks directly indicate chemical interaction between PANI nanofibres and carbon dots. As reported in the literature, FTIR spectroscopy reveals a peak at 420–700 cm^{-1} for SnO_2 corresponding to asymmetric vibration of the Sn–O bond,[51,52] while a peak at 686 cm^{-1} represents vibrations of the Sn–O–Sn bond.[52] The FTIR spectra of the PANI/CD/SnO_2 nanocomposite are similar to those of the PANI/CD (1:0.5) nanocomposite, with additional higher-intensity peaks at 688 cm^{-1}, 646 cm^{-1} and 577 cm^{-1}, which indicate that appropriate interaction of SnO_2 with PANI and CDs has occurred. This indicates that CD and SnO_2 have been perfectly incorporated into the polymer matrix, and the nanorods of SnO_2 along with CDs will function synergistically with PANI nanofibres. Fluorescence is an important characteristic of carbon dots that indicates the successful synthesis of 0D nanomaterial. A distinguishable blue colour was observed for the synthesized CDs similar to that reported in the paper from which the synthesis method was taken. The blue fluorescence along with fluorescence spectra are shown in Fig. S2.

UV–Vis spectroscopy was employed for the analysis of the interaction of the components of binary and ternary nanocomposites, that is, for pure PANI, CDs, PANI/CD (1:0.5), SnO_2, and PANI/CD/SnO_2 materials. The spectra are shown in Fig. 3d. A peak at 265 nm is obtained for pure PANI representing the π–π^* conjugated ring system, while a peak at 341 nm represents polaron π^* transitions.[53,54]

UV–Vis spectra of CDs are shown in the inset of Fig. 3d, which indicates a peak at 346 nm for the n–π^* transition.[42] From the spectra for PANI/CD, one can easily infer that CDs have been successfully incorporated and interact with PANI nanofibres. This can be seen by two peaks in the case of the PANI/CD (1:0.5) nanocomposite, which displays a peak at 265 nm, similar to that of PANI, and another at 345–346 nm, representing the resultant of 346 nm peak of CD and 341 nm peak of PANI. The higher intensity of the peak at 345–346 nm as compared to the 265 nm peak in the case of PANI/CD (1:0.5) indicates the dominance of CDs in the composite. Further investigating the absorbance of the SnO_2 nanorods, we observe a peak at 265 nm, similar to that reported in the literature.[55] The two peaks in the UV–Vis spectra of the ternary PANI/CD/SnO_2 nanocomposite demonstrate the effective interaction between the three components—PANI, CDs, and SnO_2 nanorods.

Gas Sensing Results

After having confirmed, through various characterization techniques, the successful formation of binary and ternary composites and proper interaction among the three components of the nanocomposite, it now becomes essential to examine the synthesized samples including binary and ternary composites. Hence, sensing measurements were first performed for the pristine PANI sample (p-type) towards different concentrations of ammonia gas (reducing gas) at room temperature.

As expected from the sensing interaction employed in the case of p-type material exposed to reducing gas, the resistance of the PANI-based sensor increased. This occurs because of the reduced hole concentration in p-type material (i.e. PANI) due to electron–hole recombination, where NH_3 serves as source of electrons. After some time, the resistance becomes stable, followed by a reduction in resistance of the sensor when exposed to air. Thus, this interaction of PANI with NH_3 yields responses of 7.87%, 5.66%, 5.01%, and 2.76% for 100 ppm, 75 ppm, 50 ppm, and 25 ppm NH_3, respectively, as shown in the transient response curve in Fig. 4a. In addition, response time was calculated by noting the time for the response to reach 90% of its maximum, which turned out to be 162 s, while the time taken for recovery of 90% of the response yielded a recovery time of 44 s, as shown in Fig. 4b. Further investigation was performed for all three PANI/CD nanocomposite samples with different ratios of CDs, i.e. (1:1), (1:0.5), (1:2), and compared with pure PANI for their sensing response towards different concentrations of NH_3 gas (100 ppm, 75 ppm, 50 ppm, and 25 ppm) at room temperature.

The results, as shown in Fig. 5a, indicate that the PANI/CD (1:0.5) nanocomposite yielded the highest response towards different concentrations of NH_3 compared to PANI and other samples. Hence, it can be inferred that incorporating CDs at half the amount of aniline during in situ polymerization results in the formation of an adequate number of inter-junctions between CDs and PANI nanofibres, which also helps enhance adsorption by increasing the surface area. But the incorporation of CDs in an amount equal to or double that of aniline may have led to overcrowding of the nanofibre surface, thus preventing the interaction of NH_3 molecules with PANI and resulting in a lower response, even less than that of pristine PANI. Another important parameter of sensors was then examined: selectivity towards the desired gas. Here, we tested all the samples [PANI, PANI/CD (1:1), PANI/CD (1:0.5), and PANI/CD (1:2)] for sensing ability towards 100 ppm of H_2, C_2H_5OH, CO, NO_2, and NH_3 at room temperature. The results shown in Fig. 5b clearly indicate the selective nature of the PANI/CD (1:0.5) nanocomposite towards ammonia gas as compared to other gases. The response curve for all four samples towards these different gases is given in Fig. S3. The selectivity measurements

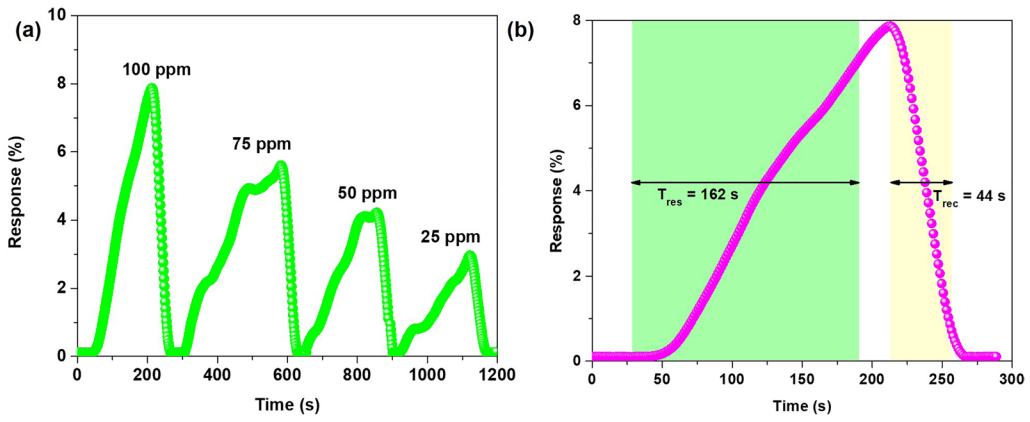

Fig. 4 (a) Transient response curve of pure PANI towards NH_3 gas (25–100 ppm) at room temperature, (b) response/recovery time for pure PANI towards 100 ppm NH_3 at room temperature.

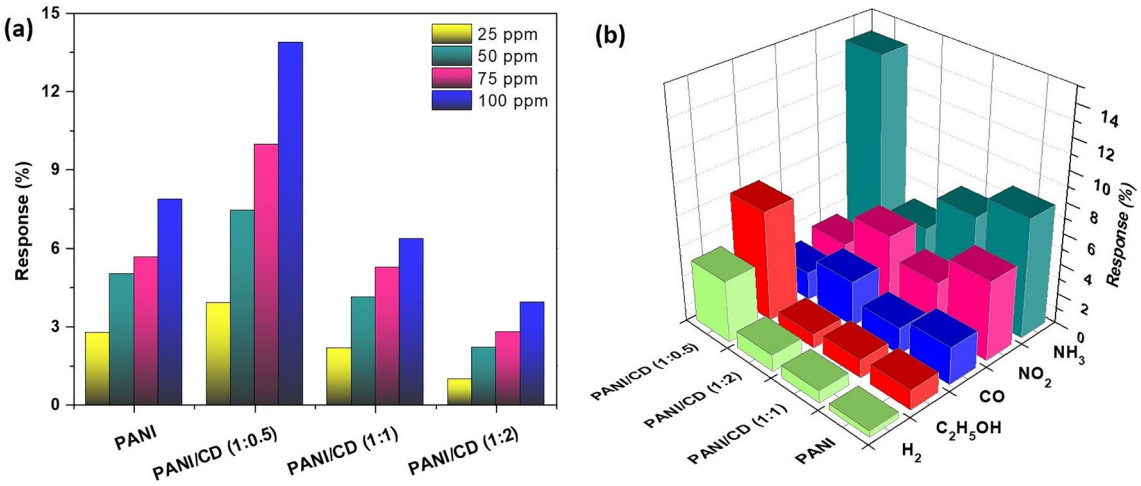

Fig. 5 (a) Comparison of the response of pure PANI and (1:1), (1:0.5), and (1:2) PANI/CD nanocomposites towards NH_3 gas (25–100 ppm) at room temperature, (b) comparison of response rate of pure PANI and (1:1), (1:0.5), and (1:2) PANI/CD nanocomposites towards 100 ppm of H_2, C_2H_5OH, CO, NO_2, and NH_3 at room temperature.

were performed for all the samples, pure PANI, and all compositions of PANI/CD nanocomposite, in which CDs were incorporated in at equal, lower, and higher amounts relative to aniline. It was observed that different samples were selective towards different gases. In general, the response of composites of different ratios of components towards different gases depends on various properties of the target analyte including its chemical structure, thermodynamic adsorption, and desorption properties with respect to the sensing material, as well as the kinetics of the target analyte. Another dominant factor responsible for differences in the response of different nanocomposites is the ratio of their components, here aniline:CD. Therefore, a possible reason for the variation in selectivity of different nanocomposites could be the different amount of CDs in different samples and their tendency to react with different gases. Hence, in the PANI/CD nanocomposite, the response will be contributed by PANI and CD both individually and synergistically, thereby producing a net response that depends on the dominance of a particular type of interaction towards the respective gas, resulting in different nanocomposites with different selectivity towards different gases, as shown in Fig. 5b. Pure PANI is selective towards ammonia gas in particular due to the possibility of protonation and deprotonation reactions between the pernigraniline and emeraldine forms of PANI. Therefore, as the amount of CDs is smaller as compared to PANI in the PANI/CD (1:0.5) nanocomposite, the dominant change in resistance is due to the interaction of PANI with NH_3 molecules, making it selective towards NH_3 gas. Hence, in the case of a lower ratio of aniline:CD, it was found to be selective towards a certain gas while a higher ratio of aniline:CD was selective for another gas.[56] Thus, the optimized ratio of CDs to be incorporated with PANI is 1:0.5 (aniline:CD), which yielded a response of 13.88% towards 100 ppm NH_3, while pure PANI, the 1:1 nanocomposite, and the 1:2 nanocomposite yielded responses of 7.87%, 6.34%, and 3.93%, respectively. The response time for the (1:0.5) PANI/CD nanocomposite was found to be 144 s, which is less than that of pure PANI. Figure S4 shows the response time for the PANI/CD (1:0.5) nanocomposite. It was observed that the nanocomposite of PANI/CD (1:0.5) exhibited the same behaviour as pristine PANI, that is, *p*-type, because its resistance increased on exposure to NH_3, similar to what occurs in pure PANI.

In order to improve the response, response time, and other parameters, further investigation was undertaken for the possibility of enhanced performance on incorporating SnO_2 metal oxide with CDs into aniline for in situ chemical oxidative polymerization. Because of the advantageous properties of SnO_2 in the context of ammonia gas sensing, the synthesized ternary nanocomposite was expected to demonstrate enhanced sensing performance relative to binary composites and pure PANI. Hence, after optimizing the amount of CDs (i.e. 1:0.5), SnO_2 nanorods at 20 wt.% of aniline were incorporated during in situ polymerization, thus forming a ternary PANI/CD/SnO_2 nanocomposite. The amount of metal oxide to be incorporated with aniline to form a binary PANI/MO nanocomposite was optimized in a previous laboratory report, which was optimized to be 20 wt.% of aniline amount used. Similarly, the amount of CDs in the binary PANI/CD nanocomposite was optimized in the present paper to be a 1:0.5 ratio. Hence, the optimized amount (20 wt.%) of SnO_2 nanorods was incorporated with the optimized ratio (1:0.5) into aniline which further polymerized in the presence of a homogeneous distribution of CDs and SnO_2 nanorods to form polyaniline nanofibres. This resulted in the successful

synthesis of the ternary PANI/CD/SnO_2 nanocomposite via in situ chemical oxidative polymerization. All other parameters were kept the same in the synthesis of pristine PANI because the aim was to analyse the improvement in sensing performance of a sensing material that involves mutually interacting components of PANI, CDs, and SnO_2 over a pristine sensing material (PANI) with no other components.

Upon exposure of the ternary nanocomposite to ammonia gas at concentrations of 100 ppm, 75 ppm, 50 ppm, 25 ppm, 10 ppm, and 5 ppm at room temperature, the resistance of the ternary nanocomposite was observed to increase for ammonia as compared to that in air, as can be seen in Fig. 6a.

As ammonia is a reducing gas, it was considered that the PANI/CD/SnO_2 nanocomposite would have the same behaviour as pristine PANI, that is, *p*-type. Based on the observed data, the response was calculated as shown in Fig. 6b. The ternary nanocomposite exhibited 21.6% response towards 100 ppm NH_3, which is higher than pure PANI and the binary PANI/CD nanocomposite, as expected, which achieved 7.87% and 13.88%, respectively, towards the same concentration of gas. A response time of 94 s was calculated for PANI/CD/SnO_2 for 100 ppm NH_3, as shown in Fig. 6c, highlighting the considerably reduced response time for the ternary nanocomposite towards 100 ppm NH_3 as compared to that for both pure PANI (162 s) and the PANI/CD (1:0.5) nanocomposite (144 s). However, the recovery time of the composite increased to 459 s. The response rate was further analysed on increasing the gas/analyte concentration, as shown in Fig. 6d. The response rate of the ternary nanocomposite exhibited an almost linear relationship with the concentration of ammonia gas. Also, the lower limit of detection was improved, as the sensing material displayed an excellent response even for 5 ppm NH_3 gas.

A sensing material can be regarded as appropriate for sensor fabrication only if it is highly selective towards the desired gas, in our case ammonia, over other gases. This is important when considering practical applications in which a sensor should be responsive only towards the target analyte even in the presence of an abundance of other gases. As shown in Fig. 7a, when the ternary nanocomposite was exposed to 100 ppm of C_2H_5OH, CO_2, H_2, and NO_2, low response of 0.64%, 1.21%, 0.69%, and 6.58%, respectively, was observed, which was much lower than the response of 21.6% towards the same concentration of NH_3 gas, as

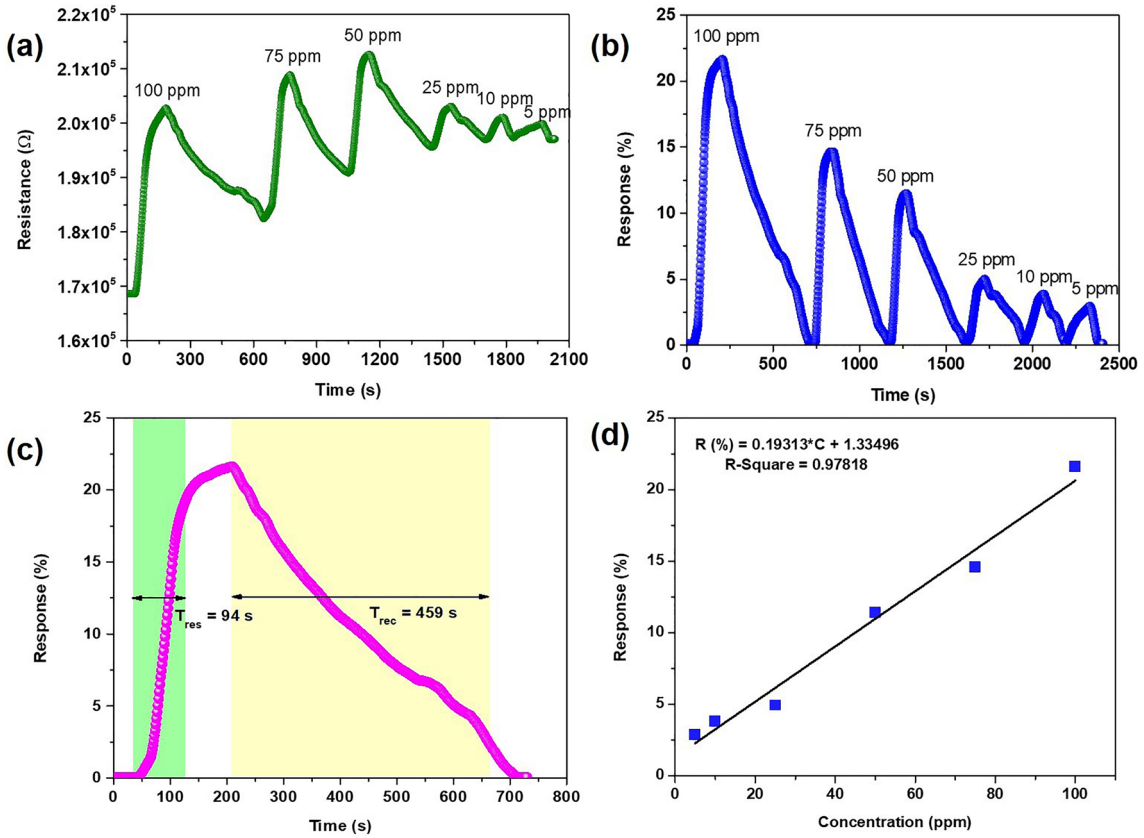

Fig. 6 (a) Transient resistance curve for the ternary PANI/CD/SnO_2 nanocomposite towards 5–100 ppm NH_3 gas at room temperature, (b) dynamic response curve for the ternary PANI/CD/SnO_2 nanocomposite towards 5–100 ppm NH_3 gas at room temperature, (c) response/recovery time for the PANI/CD/SnO_2 nanocomposite towards 100 ppm NH_3 at room temperature, (d) response versus concentration of NH_3 for the PANI/CD/SnO_2 nanocomposite.

desired. The response curve for 100 ppm of different gases is shown in the inset of Fig. 7a. This highlights the highly selective nature of the PANI/CD/SnO_2 nanocomposite towards NH_3 gas over other gases, which makes it a preferred option for ammonia gas sensing.

Another important parameter, repeatability, was examined for the PANI/CD/SnO_2 nanocomposite over 10 cycles of 25 ppm NH_3 gas, and the composite was found to produce sufficient repeatability, as shown in Fig. 7b. Hence, this sensor demonstrates both high stability and good repeatability, making the sensing material (PANI/CD/SnO_2 nanocomposite) a good candidate for use in practical applications.

Very few studies have investigated ternary composites for ammonia sensing. Table I shows a comparison of the sensing parameters of these different types of sensing materials for ammonia gas sensing at room temperature.

The significance of the ternary PANI/CD/SnO_2 nanocomposite can be observed in terms of the improvement not only in the sensitivity (improved from 7.87% to 21.6%) and selectivity towards ammonia gas but also in the lower limit of detection, which is significantly reduced to 5 ppm. The most important advantage of the sensing material reported in this paper is the one-step in situ method of synthesis of the ternary PANI/CD/SnO_2 nanocomposite, which is easier to perform than other reported nanocomposites. Also, the components of the nanocomposite including CDs and SnO_2 nanorods are synthesized via easy and efficient methods, making the complete synthesis a facile process. Therefore, this combination of components comprising PANI, CDs, and SnO_2 in the form of a nanocomposite, which to the best of our knowledge has never been reported for ammonia sensing, is a valuable contribution to the field of gas sensors in terms of its sensing properties and synthesis techniques.

Gas Sensing Mechanism

PANI nanofibres exhibit efficient sensing of ammonia based on the protonation/deprotonation mechanism (doping).[59] On exposure of the PANI nanofibre to NH_3, protonation of NH_3 occurs, forming an NH_4^+ ion, while deprotonation of PANI (emeraldine) occurs, resulting in the pernigraniline form of PANI (fully oxidized form). This leads to a reduction in proton concentration (majority charge carriers) in the polyaniline molecule (*p*-type) and results in increased resistance of PANI nanofibres on exposure to NH_3 gas. The doping reaction is reversible, meaning that the proton returns to the PANI molecule when exposed to air, because the air molecule takes up the hydrogen from the NH_4^+ ion. This

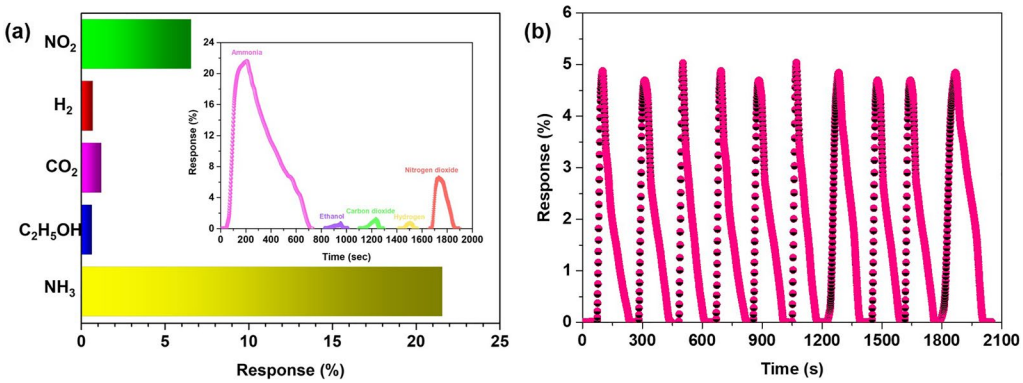

Fig. 7 (a) Comparison of response rate for the PANI/CD/SnO_2 nanocomposite towards 100 ppm of C_2H_5OH, CO_2, H_2, NO_2, and NH_3 gas at room temperature; (b) repeated measurements of response rate for the PANI/CD/SnO_2 nanocomposite towards 25 ppm of NH_3 gas at room temperature over 10 cycles.

Table I Comparison of different composite sensing materials for ammonia gas sensing at room temperature

Material	Synthesis method	Concentration (ppm)	Response (%)	Response time (s)	Refs.
PANI/SnO_2	Physical mixing	4	1.5	44	35
Sn-TiO_2@rGO/CNT	Solvothermal	250	85.9	99	26
PANI/hollow C#In_2O_3	In situ chemical oxidative polymerization	1	17.8	~530	22
PANI/rGO/SnO_2	Solvothermal	100	45	45	57
SWCNTs-OH/PANI	In situ polymerization	100	2	93	58
PANI/CD/SnO_2	In situ chemical oxidative polymerization	100	21.6	94	This work

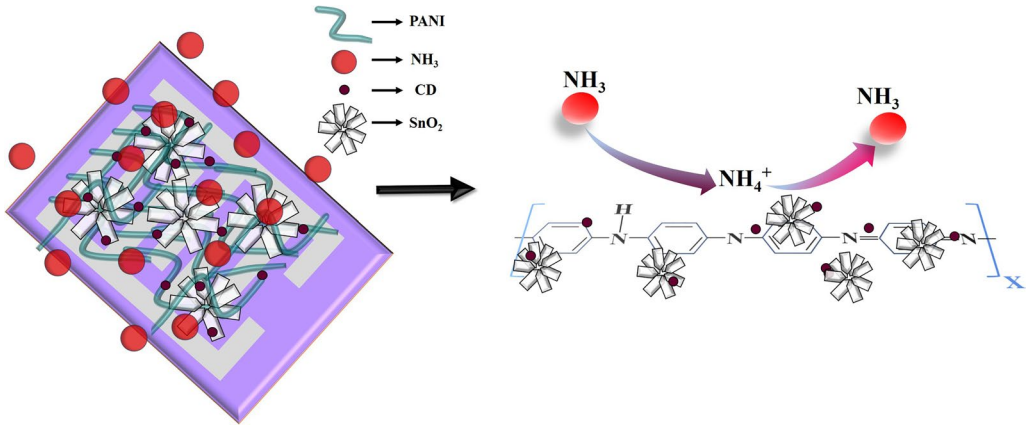

Fig. 8 Schematic for mechanism of ammonia gas molecule interaction with the ternary composite material.

causes the resistance of PANI nanofibres to decrease back to the initial value and initial form. The doping process is explained by means of chemical reaction as[59]

$$\text{PANI} - \text{H}^+ \rightarrow \text{PANI} + \text{NH}_4^+$$

Carbon dots are 0D structures offering a high surface-to-volume ratio for higher adsorption of gas molecules, thereby increasing the specific area when incorporated to form the binary PANI/CD nanocomposite and hence facilitating an increase in the interaction sites of NH_3 with the sensing material.[38] It has also been observed that the initial resistance of the PANI/CD composite in air is higher than that of pure PANI, which indicates that CDs have interacted well with PANI nanofibres. This might facilitate the enhanced response of the binary nanocomposite over pure PANI. As observed, the PANI/CD nanocomposite behaves as a *p*-type material; hence the majority charge carriers (holes) are depleted on exposure to NH_3, as reducing gas, where CDs might be aid in hole depletion from the sensing material.

SnO_2 metal oxide is an *n*-type material and forms a p–n heterojunction with *p*-type PANI/CD, thus producing a depletion layer between the two, whose width changes when exposed to reducing gas.[40] The enhance sensing response of the PANI/CD/SnO_2 nanocomposite relative to pure PANI and the PANI/CD nanocomposite can be attributed to the increased specific surface area on incorporation of both CDs and SnO_2 nanorods, as well as the synergistic effect of all three components, which individually are adequately responsive towards ammonia gas in pure or binary form. The initial resistance of the PANI/CD/SnO_2 composite is lower than that of both pure PANI and the PANI/CD binary composite, and it is observed to exhibit *p*-type behaviour similar to PANI. Hence, the increased conductivity might play a role in the improved response. Also, the possibility of heterojunction formation between *p*-type PANI/CD and *n*-type SnO_2 can be considered as an important factor that might be responsible for the increased response. It facilitates the easy adsorption of NH_3 molecules, which can exchange charge carriers in a similar way as with pure PANI but now in increased numbers due to the increase in majority charge carriers as well as the additional force facilitating the flow of charge carriers along the conductive pathway formed as a result of the interaction of all three nanocomposites. This exchange of a larger number of charge carriers produces a greater change in resistance and hence better response towards the same concentration of gas. Also, the highly entangled structure of the ternary nanocomposite, as visible in SEM images, plays a role in increased adsorption because of the possibility that ammonia gas molecules will enter the empty spaces and interact with more of the surface area. A schematic representation of the fabricated gas sensor based on the ternary PANI/CD/SnO_2 nanocomposite along with its interaction with ammonia gas molecules is shown in Fig. 8.

Conclusion

In conclusion, the purpose of this paper was to explore the effect of incorporating a carbon-based 0D nanoparticle (carbon dots) into a polymer matrix (PANI nanofibres) via in situ polymerization and to further analyse the role of metal oxide (SnO_2) when incorporated along with CDs into the PANI matrix, enabling an understanding of the response mechanism of the ternary nanocomposite. First, the effect of incorporating different amounts of CDs was analysed, as a result of which we optimized the ratio of aniline:CDs as 1:0.5 giving the highest response of 13.88% towards 100 ppm NH_3 gas as compared to pure PANI (1:1) and (1:2) PANI/CD nanocomposites. In addition, SnO_2 nanorods of a previously optimized amount (20 wt.%) were incorporated via in situ polymerization to form the ternary PANI/CD/

SnO_2 nanocomposite. This particular ternary PANI/CD/SnO_2 nanocomposite is reported herein for the first time for ammonia gas sensing and proved to be a good option for practical real-life application in ammonia gas sensing due to the improved sensing parameters. These include a higher response of 21.6% towards 100 ppm NH_3 gas with a lower detection limit of 5 ppm and lower response time of 94 s. The improved response and response time of the ternary PANI/CD/SnO_2 nanocomposite (21.6%, 94 s) over those of both the binary PANI/CD (1:0.5) nanocomposite (13.88%, 144 s) and pure PANI (7.87%, 162 s) highlight the fact that combining three sensing materials, with their respective advantages which counter the disadvantages of the others, is an important and valuable technique for fabricating improved sensors. The most important feature of this nanocomposite is its high selectivity towards NH_3 gas over other gases including C_2H_5OH, CO_2, H_2, and NO_2. Good repeatability and long-term stability provide advantages for the fabrication of ammonia gas sensors based on this ternary PANI/CD/SnO_2 nanocomposite. The successful synthesis of the binary nanocomposite was confirmed through different characterization techniques including SEM, FTIR spectroscopy, Raman spectroscopy, UV–Vis spectroscopy, and XRD.

Supplementary Information The online version contains supplementary material available at https://doi.org/10.1007/s11664-024-11168-9.

Conflict of interest On behalf of all authors, the corresponding author states that there is no conflict of interest.

References

1. M. Zulkifli, H. Abu Hasan, S.R. Sheikh Abdullah, and M.H. Muhamad, A review of ammonia removal using a biofilm-based reactor and its challenges. *J. Environ. Manag.* 315, 115162 (2022).
2. S.D. Lawaniya, S. Kumar, Y. Yu, and K. Awasthi, Ammonia sensing properties of PPy nanostructures (urchins/flowers) towards low-cost and flexible gas sensors at room temperature. *Sens. Actuators B Chem.* 382, 133566 (2023).
3. X. Wang, S. Meng, M. Tebyetekerwa, W. Weng, J. Pionteck, B. Sun, Z. Qin, and M. Zhu, Nanostructured polyaniline/poly(styrene-butadiene-styrene) composite fiber for use as highly sensitive and flexible ammonia sensor. *Synth. Met.* 233, 86 (2017).
4. S.D. Lawaniya, N. Meena, S. Kumar, Y.-T. Yu, and K. Awasthi, Effect of MWCNTs incorporation into polypyrrole (PPy) on ammonia sensing at room temperature. *IEEE Sens. J.* 23, 1837 (2023).
5. R.P. Padappayil and J. Borger, *Ammonia Toxicity* (St. Petersburg: StatPearls, 2024).
6. Y. Li, L. Pan, X. Zeng, R. Zhang, X. Li, J. Li, H. Xing, and J. Bao, Ammonia exposure causes the imbalance of the gut-brain axis by altering gene networks associated with oxidative metabolism, inflammation and apoptosis. *Ecotoxicol. Environ. Saf.* 224, 112668 (2021).
7. M.-J. Chan, Y.-J. Li, C.-C. Wu, Y.-C. Lee, H.-W. Zan, H.-F. Meng, M.-H. Hsieh, C.-S. Lai, and Y.-C. Tian, Breath ammonia is a useful biomarker predicting kidney function in chronic kidney disease patients. *Biomedicines* 8, 468 (2020).
8. T. Hibbard and A.J. Killard, Breath ammonia analysis: clinical application and measurement. *Crit. Rev. Anal. Chem.* 41, 21 (2011).
9. M. Poloju, N. Jayababu, and M.V. RamanaReddy, Improved gas sensing performance of Al doped ZnO/CuO nanocomposite based ammonia gas sensor. *Mater. Sci. Eng. B* 227, 61 (2018).
10. S.D. Lawaniya, S. Kumar, Y. Yu, and K. Awasthi, Flexible, low-cost, and room temperature ammonia sensor based on polypyrrole and functionalized MWCNT nanocomposites in extreme bending conditions. *ACS Appl. Polym. Mater.* 5, 1945 (2023).
11. A. Husain, S. Ahmad, M.U. Shariq, and M.M.A. Khan, Ultrasensitive, highly selective and completely reversible ammonia sensor based on polythiophene/SWCNT nanocomposite. *Materialia* 10, 100704 (2020).
12. S.D. Lawaniya, S. Kumar, Y. Yu, H.-G. Rubahn, Y.K. Mishra, and K. Awasthi, Functional nanomaterials in flexible gas sensors: recent progress and future prospects. *Mater. Today Chem.* 29, 101428 (2023).
13. X. Liu, W. Zheng, R. Kumar, M. Kumar, and J. Zhang, Conducting polymer-based nanostructures for gas sensors. *Coord. Chem. Rev.* 462, 214517 (2022).
14 N.L. Torad and M.M. Ayad, *Gas Sensors Based on Conducting Polymers* (London: IntechOpen, 2019).
15. C. Bavatharani, E. Muthusankar, S.M. Wabaidur, Z.A. Alothman, K.M. Alsheetan, M. Mana AL-Anazy, and D. Ragupathy, Electrospinning technique for production of polyaniline nanocomposites/nanofibres for multi-functional applications: a review. *Synth. Met.* 271, 116609 (2021).
16. J. Cai, C. Zhang, A. Khan, C. Liang, and W.-D. Li, Highly transparent and flexible polyaniline mesh sensor for chemiresistive sensing of ammonia gas. *RSC Adv.* 8, 5312 (2018).
17. A. Qureshi, A. Altindal, and A. Mergen, Electrical and gas sensing properties of Li and Ti codoped NiO/PVDF thin film. *Sens. Actuators B Chem.* 138, 71 (2009).
18 S.D. Lawaniya, S. Kumar, Y. Yu, Y.K. Mishra, and K. Awasthi, *Complex and Composite Metal Oxides for Gas VOC and Humidity Sensors Volume 1* (Amsterdam: Elsevier, 2024), pp.107–150.
19. A. Eatemadi, H. Daraee, H. Karimkhanloo, M. Kouhi, N. Zarghami, A. Akbarzadeh, M. Abasi, Y. Hanifehpour, and S.W. Joo, Carbon nanotubes: properties, synthesis, purification, and medical applications. *Nanoscale Res. Lett.* 9, 393 (2014).
20. N. Nath, A. Kumar, S. Chakroborty, S. Soren, A. Barik, K. Pal, and F.G. de Souza, Carbon nanostructure embedded novel sensor implementation for detection of aromatic volatile organic compounds: an organized review. *ACS Omega* 8, 4436 (2023).
21. P. Dariyal, S. Sharma, G.S. Chauhan, B.P. Singh, and S.R. Dhakate, Recent trends in gas sensing via carbon nanomaterials: outlook and challenges. *Nanoscale Adv.* 3, 6514 (2021).
22. S.-Z. Hong, Q.-Y. Huang, and T.-M. Wu, Facile synthesis of polyaniline/carbon-coated hollow indium oxide nanofiber composite with highly sensitive ammonia gas sensor at the room temperature. *Sensors* 22, 1570 (2022).
23. S.D. Lawaniya, S. Kumar, Y. Yu, and K. Awasthi, Nitrogen-doped carbon nano-onions/polypyrrole nanocomposite based low-cost flexible sensor for room temperature ammonia detection. *Sci. Rep.* 14, 7904 (2024).
24. L.A. Panes-Ruiz, M. Shaygan, Y. Fu, Y. Liu, V. Khavrus, S. Oswald, T. Gemming, L. Baraban, V. Bezugly, and G. Cuniberti, Toward highly sensitive and energy efficient ammonia gas detection with modified single-walled carbon nanotubes at room temperature. *ACS Sens.* 3, 79 (2018).
25. W. Muangrat, W. Wongwiriyapan, V. Yordsri, T. Chobsilp, S. Inpaeng, C. Issro, O. Domanov, P. Ayala, T. Pichler, and L. Shi, Unravel the active site in nitrogen-doped double-walled carbon

nanotubes for nitrogen dioxide gas sensor. *Phys. Status Solidi* (2018). https://doi.org/10.1002/pssa.201800004.
26. Y. Seekaew, W. Pon-On, and C. Wongchoosuk, Ultrahigh selective room-temperature ammonia gas sensor based on tin–titanium dioxide/reduced graphene/carbon nanotube nanocomposites by the solvothermal method. *ACS Omega* 4, 16916 (2019).
27. R. Ghosh, A. Midya, S. Santra, S.K. Ray, and P.K. Guha, Chemically reduced graphene oxide for ammonia detection at room temperature. *ACS Appl. Mater. Interfaces* 5, 7599 (2013).
28. O. Tsymbalenko, S. Lee, Y.-M. Lee, Y.-S. Nam, B.C. Kim, J.Y. Kim, and K.-B. Lee, High-sensitivity NH_3 gas sensor using pristine graphene doped with CuO nanoparticles. *Microchim. Acta* 190, 134 (2023).
29. Z. Wu, X. Chen, S. Zhu, Z. Zhou, Y. Yao, W. Quan, and B. Liu, Enhanced sensitivity of ammonia sensor using graphene/polyaniline nanocomposite. *Sens .Actuators B Chem.* 178, 485 (2013).
30. R. Paul, B. Das, and R. Ghosh, Novel approaches towards design of metal oxide based hetero-structures for room temperature gas sensor and its sensing mechanism: a recent progress. *J. Alloys Compd.* 941, 168943 (2023).
31. J.N. Gavgani, H.S. Dehsari, A. Hasani, M. Mahyari, E.K. Shalamzari, A. Salehi, and F.A. Taromi, A room temperature volatile organic compound sensor with enhanced performance, fast response and recovery based on N-doped graphene quantum dots and poly(3,4-ethylenedioxythiophene)–poly(styrenesulfonate) nanocomposite. *RSC Adv.* 5, 57559 (2015).
32. M. Hakimi, A. Salehi, F.A. Boroumand, and N. Mosleh, Fabrication of a room temperature ammonia gas sensor based on polyaniline With N-doped graphene quantum dots. *IEEE Sens. J.* 18, 2245 (2018).
33. J.N. Gavgani, A. Hasani, M. Nouri, M. Mahyari, and A. Salehi, Highly sensitive and flexible ammonia sensor based on S and N co-doped graphene quantum dots/polyaniline hybrid at room temperature. *Sens. Actuators B Chem.* 229, 239 (2016).
34. Y. Qin, X. Liu, and J. Xie, Humidity-enhanced NH_3 sensor based on carbon quantum dots-modified SnS. *Appl. Surf. Sci.* 634, 157612 (2023).
35. Q. Feng, H. Zhang, Y. Shi, X. Yu, and G. Lan, Preparation and gas sensing properties of PANI/SnO_2 hybrid material. *Polymers (Basel)* 13, 1360 (2021).
36. S. Dua, P. Kumar, B. Pani, A. Kaur, M. Khanna, and G. Bhatt, Stability of carbon quantum dots: a critical review. *RSC Adv.* 13, 13845 (2023).
37. R. Kaur, S.D. Lawaniya, S. Kumar, N. Saini, and K. Awasthi, Nanoarchitectonics of polyaniline–zinc oxide (PANI–ZnO) nanocomposite for enhanced room temperature ammonia sensing. *Appl. Phys. A* 129, 765 (2023).
38. S.-Z. Hong, Q.-Y. Huang, and T.-M. Wu, The room temperature highly sensitive ammonia gas sensor based on polyaniline and nitrogen-doped graphene quantum dot-coated hollow indium oxide nanofiber composite. *Polymers (Basel)* 13, 3676 (2021).
39. C.-H. Hsieh, L.-H. Xu, J.-M. Wang, and T.-M. Wu, Fabrication of polypyrrole/tin oxide/graphene nanoribbon ternary nanocomposite and its high-performance ammonia gas sensing at room temperature. *Mater. Sci. Eng. B* 272, 115317 (2021).
40. S.K. Gautam, N.A. Gokhale, and S. Panda, Mechanism of NH_3 gas sensing by SnO_2/PANI nanocomposites: charge transport and temperature dependence study. *Flex. Print. Electron.* 7, 035022 (2022).
41. P.G. Choi, A. Tsuruta, and Y. Masuda, Nanosheet-type tin oxide on carbon nanotube for gas sensing. *Chem. Eng. J.* 472, 144799 (2023).
42. K. Holá, M. Sudolská, S. Kalytchuk, D. Nachtigallová, A.L. Rogach, M. Otyepka, and R. Zbořil, Graphitic nitrogen triggers red fluorescence in carbon dots. *ACS Nano* 11, 12402 (2017).
43. G. Pandey, S.D. Lawaniya, S. Kumar, P.K. Dwivedi, and K. Awasthi, A highly selective, efficient hydrogen gas sensor based on bimetallic (Pd–Au) alloy nanoparticle (NP)-decorated SnO_2 nanorods. *J. Mater. Chem. A* 11, 26687 (2023).
44. A. Kumar, V. Kumar, P.K. Sain, M. Kumar, and K. Awasthi, Synthesis and characterization of polyaniline membranes with—secondary amine additive containing N, N′-dimethyl propylene urea for fuel cell application. *Int. J. Hydrog. EnergyHydrog. Energy* 43, 21715 (2018).
45. A.F. Shaikh, M.S. Tamboli, R.H. Patil, A. Bhan, J.D. Ambekar, and B.B. Kale, Bioinspired carbon quantum dots: an antibiofilm agents. *J. Nanosci. Nanotechnol.* 19, 2339 (2019).
46. A.I. Fatya, M. Reza, R.R. Sunarya, and V. Suendo, Synthesis of polyaniline/electrochemically exfoliated graphene composite as counter-electrode in dye-sensitized solar cell. *Polym. Technol. Mater.* 59, 1370 (2020).
47. H. Salah Abdullah, Electrochemical polymerization and Raman study of polypyrrole and polyaniline thin films. *Int. J. Phys. Sci.* 7, 5468 (2012).
48. H. Wang, Q. Hao, X. Yang, L. Lu, and X. Wang, Effect of graphene oxide on the properties of its composite with polyaniline. *ACS Appl. Mater. Interfaces* 2, 821 (2010).
49. Z. Li, Y. Shen, Y. Li, F. Zheng, L. Liu, X. Liu, and D. Zou, Preparation of polyaniline hollow microspheres/zinc composite and its application in lithium battery. *High Perform. Polym.* 31, 178 (2019).
50. H. Zhu, S. Peng, and W. Jiang, Electrochemical properties of PANI as single electrode of electrochemical capacitors in acid electrolytes. *Sci. World J.* 2013, 1 (2013).
51. F. Kurniawan and R. Rahmi, Synthesis of SnO_2 nanoparticles by high potential electrolysis. *Bull. Chem. React. Eng. Catal.* 12, 281 (2017).
52. S.A. Saleh, A.A. Ibrahim, and S.H. Mohamed, Structural and optical properties of nanostructured Fe-doped SnO_2. *Acta Phys. Pol. A* 129, 1220 (2016).
53. M. Alam, N.M. Alandis, A.A. Ansari, and M.R. Shaik, Optical and electrical studies of polyaniline/ZnO nanocomposite. *J. Nanomater.* 2013, 1 (2013).
54. F. Habtamu, S. Berhanu, and T. Mender, Polyaniline supported Ag-doped ZnO nanocomposite: synthesis, characterization, and kinetics study for photocatalytic degradation of malachite green. *J. Chem.* 2021, 1 (2021).
55. J.O. Adeyemi and D.C. Onwudiwe, SnS_2 and SnO_2 nanoparticles obtained from organotin(IV) dithiocarbamate complex and their photocatalytic activities on methylene blue. *Materials (Basel)* 13, 2766 (2020).
56. K.A. Mirica, J.M. Azzarelli, J.G. Weis, J.M. Schnorr, and T.M. Swager, Rapid prototyping of carbon-based chemiresistive gas sensors on paper. *Proc. Natl. Acad. Sci.* (2013). https://doi.org/10.1073/pnas.1307251110.
57. K.K. Saravanan, P. Siva Karthik, P.R. Mirtha, J. Balaji, and B. Rajeshkanna, A one-pot hydrothermal-induced PANI/SnO_2 and PANI/SnO_2/rGO ternary composites for high-performance chemiresistive-based H_2S and NH_3 gas sensors. *J. Mater. Sci. Mater. Electron.* 31, 8825 (2020).
58. X. Chen, X. Chen, X. Ding, X. Yu, and X. Yu, Enhanced ammonia sensitive properties and mechanism research of PANI modified with hydroxylated single-walled nanotubes. *Mater. Chem. Phys.* 226, 378 (2019).
59. S.B. Kulkarni, Y.H. Navale, S.T. Navale, F.J. Stadler, and V.B. Patil, Room temperature ammonia gas sensing properties of polyaniline nanofibers. *J. Mater. Sci. Mater. Electron.* 30, 8371 (2019).